JCAMECH

Vol. 48, No. 1, June 2017, pp 123-136
DOI: 10.22059/jcamech.2017.236217.155

Refined plate theory for free vibration analysis of FG nanoplates using the nonlocal continuum plate model

M. Goodarzi[1,*], M. Nikkhah Bahrami[2], V. Tavaf [3]

[1]*Department of Mechanical Engineering, Ahvaz Branch, Islamic Azad University, Ahvaz, Iran*

[2]*Department of Engineering, Science and Research Branch, Islamic Azad University, Tehran, Iran*

[3]*Department of Mechanical Engineering at University of South Carolina, Columbia, USA*

Received: 21 Apr. 2017, Accepted: 27 June. 2017

Abstract

In this article, the free vibration behavior of nanoscale FG rectangular plates is studied within the framework of the refined plate theory (RPT) and small-scale effects are taken into account. Using the nonlocal elasticity theory, the governing equations are derived for single-layered FG nanoplate. The Navier's method is employed to obtain closed-form solutions for rectangular nanoplates assuming that all edges are simply supported. The results are subsequently compared with valid results reported in the literature. The effects of the small scale on natural frequencies are investigated considering various parameters such as aspect ratio, thickness ratio, and mode numbers. It is shown that the RPT is an accurate and simple theory for the vibration analysis of nanoplates, which does not require a shear correction factor.

Keywords: *Small scale, refined plate theory, vibration analysis, FGM nanoplate.*

1. Introduction

Over the past two decades, many researchers have employed the nonlocal elasticity theory for the investigation of the vibration behavior and buckling response of nanostructures. Such nanostructures include nanotubes[1-5], nanorods[6], nanorings[7]and nanoplates [8-14]. The nonlocal elasticity theory was introduced by Eringen [15]. He modified the classical continuum mechanics for taking into account small scale effects. In this theory, the stress state at a given point depends on the strain states at all points in the domain, while in the local theory, the stress state at any given point depends only on the strain state at that point.

Graphene is a truly two-dimensional atomic crystal with exceptional electronic and mechanical properties.

* Corresponding Author. Tel.: +98 9163004640; Fax: +98 6134448049
Email Address: mz.goodarzi@gmail.com

The graphene sheets are widely used in the micro electro-mechanical systems (MEMS), nano electro-mechanical systems (NEMS), and in devices such as oscillators, clocks, and sensors. Electromechanical resonators are NEMS devices made from suspended single- and multi-layered graphene sheets [16]. Furthermore, potential applications have been investigated for the SLGSs as mass sensors and atomistic dust detectors [17]. Proper application of SLGSs depends on a thorough understanding of their mechanical properties. Vibration behavior is one such mechanical property that is of great importance from a design perspective. Ansari[18] obtained the natural frequencies of a multi-layered graphene sheet embedded in an elastic medium. The vibration analysis of the circular nanoplate was investigated by researchers[13]. Theclassical plate theory (CPT) and first-order shear deformation theory (FSDT) were developed for the free vibration of nanoplates [19].Aghababaei and Reddy[19] reformulated the third-order shear deformation plate theory for the vibration and bending of nanoplates. Ansari et al.[18]investigated the vibrational characteristics of multi-layered graphene sheets using the nonlocal finite element model. Assadi and Farshi [20] studied the free vibration of circular nanoplates taking into accounttheir surface properties. A levy type method has also been used in the vibration and buckling analysis of nanoplates using the nonlocal plate model [10].

In this paper the refined plate theory is applied to obtain the vibration frequency of the FG rectangular nanoplate. The transverse displacement has two (bending and shear) components and the parabolic distribution of the transverse shear strains through the thickness of the plate is taken into account. In this theory, it is assumed that the transverse shear strains vary parabolically across the thickness. The shear stress components satisfy the zero traction boundary conditions on the top and bottom surfaces of the plate without using shear correction factors. In the present work, RPT has been extended to single-layered graphene sheets. The governing equations are derived for the FG rectangular nanoplate based on the nonlocal elasticity theory. Explicit solutions are obtained for the natural frequencies of rectangular nanoplates with all edges simply supported by applying the Navier's method. The natural frequencies calculated by the proposed theory are compared with results obtained from other theories such as the classical plate theory (CPT), first order shear deformation theory (FSDT), and third order shear deformation theory (TSDT). The effects of the small scale on natural frequencies are also studiedby considering various parameters such as aspect ratio, thickness ratio, and mode numbers.

2. Nonlocal elasticity

As mentioned in the previous Section, the nonlocal elasticity theory, first introduced by Eringen [21], has been widely used for the analysis of nonlocal problems [12, 22-28]. According to this theory, a stress-strain relationship for a homogeneous elastic solid is expressed as:

$$\sigma_{ij} = \iiint_V \varphi(\left|x - x'\right|, \eta)\sigma_{ij}^{l} dV \tag{1}$$

where, σ_{ij} and σ_{ij}^{l} are the nonlocal and local stress tensors, respectively. The integration extends over the entire body volume, V. The function φ is the nonlocal modulus, which contains the small scale effects. It is obvious that the nonlocal modulus has the dimension of $(length)^{-3}$. This function depends on two variables, namely $\left|x - x'\right|$ and η, as seen from the above equation. $\left|x - x'\right|$ represents the distance between points x and x'. η is a material constant defined by:

$$\eta = \frac{e_0 l_i}{L} \tag{2}$$

where, l_i and L denote the internal and external characteristic lengths, respectively. The value of the parameter e_0 is vital for the validity of nonlocal models. Eringen [21] obtained a value of 0.39 for this parameter by matching the dispersion curves based on atomic models. Recently, most researchers have used values ranging from 0 to 2 nm for the nonlocal parameter, $e_0 l_i$,in the analysis of nanoplates.

It is difficult to apply Eq. (1) for solving nonlocal elasticity problems. Therefore, the following differential form of Eq. (2) is often used [29]

$$\sigma_{ij} - (e_0 a)^2 \nabla^2 \sigma_{ij} = C : \varepsilon \tag{3}$$

The symbol ':' indicates the double dot product, while C and ε are the fourth order elasticity and strain tensors, respectively. $\nabla^2 = \partial^2/\partial x^2 + \partial^2/\partial y^2$ is the two-dimensional Laplace operator. Note that the classical relationship between the stress and strain tensors can be obtained by setting $e_0 a = 0$ in the above constitutive equation. The local stress tensor is as follows:

3. Governing equations based on RPT

In the present work, we employ the refined plate theory for the vibration analysis of rectangular nanoplates (Fig. 1). According to this theory, the transverse shear strains vary parabolically over the plate thickness. The shear stress components must satisfy the following conditions:

$$\tau_{xz}=\tau_{yz}=0 \quad \text{at} \quad z=\pm\frac{h}{2} \tag{4}$$

where, h is plate thickness.

The displacement field can be written as:

$$U(x,y,z,t)=u(x,y,t)-z\frac{\partial w_b}{\partial x}-zf_1(z)\frac{\partial w_s}{\partial x}$$
$$V(x,y,z,t)=v(x,y,t)-z\frac{\partial w_b}{\partial y}-zf_2(z)\frac{\partial w_s}{\partial y}$$
$$W(x,y,z,t)=w_e(x,y,t)+w_b(x,y,t)+w_s(x,y,t) \tag{5}$$

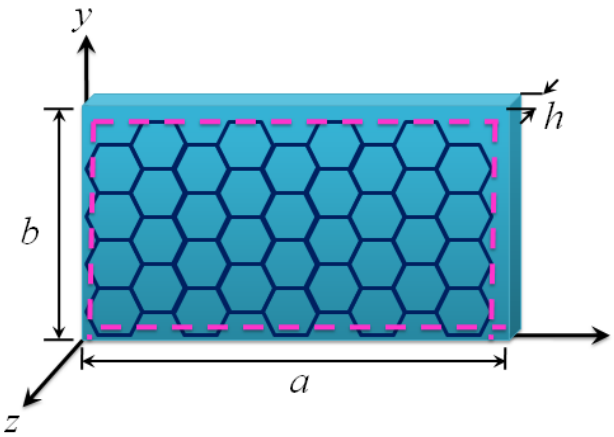

Fig.1.A continuum plate model of the nanoplate.

where,

$$f_1(z)=\frac{5}{3}\left(\frac{z}{h}\right)^2-\frac{1}{4}, \quad f_2(z)=\frac{5}{4}-5\left(\frac{z}{h}\right)^2 \tag{6}$$

in which, u and v denote mid-plane displacements of the plate in the x and y directions, respectively. w_e, w_b, and w_s represent the extension, bending, and shear components of *the* transverse displacement, respectively. The extension component w_e of the transverse displacement may be regarded as negligible compared to other displacement components in most cases. Using the above-mentioned displacement field, one can obtain the strains as follows:

$$\{\varepsilon\}=\{\varepsilon^0\}+z\{\kappa^b\}+zf_1(z)\{\kappa^s\}$$
$$\{\gamma\}=\{\chi^e\}+f_2(z)\{\chi^s\} \tag{7}$$

where,

$$\{\varepsilon\}=\left[\varepsilon_x,\varepsilon_y,\gamma_{xy}\right]^T,\ \{\varepsilon^0\}=\left[\frac{\partial u}{\partial x},\frac{\partial v}{\partial y},\left(\frac{\partial u}{\partial y}+\frac{\partial v}{\partial x}\right)\right]^T,$$
$$\{\kappa^b\}=-\left[\frac{\partial^2 w_b}{\partial x^2},\frac{\partial^2 w_b}{\partial y^2},2\frac{\partial^2 w_b}{\partial x\partial y}\right]^T$$
$$\{\kappa^s\}=-\left[\frac{\partial^2 w_s}{\partial x^2},\frac{\partial^2 w_s}{\partial y^2},2\frac{\partial^2 w_s}{\partial x\partial y}\right]^T,\ \{\gamma\}=\begin{Bmatrix}\gamma_{yz}\\ \gamma_{xz}\end{Bmatrix},$$
$$\{\chi^e\}=\left[\frac{\partial w_e}{\partial y},\frac{\partial w_e}{\partial x}\right]^T,\ \{\chi^s\}=\left[\frac{\partial w_s}{\partial y},\frac{\partial w_s}{\partial x}\right]^T \tag{8}$$

The resultant stresses N, M, and Q are defined by

$$\left(M_x^b,M_y^b,M_{xy}^b\right)=\int_{-h/2}^{h/2}\left(\sigma_x,\sigma_y,\sigma_z\right)zdz \tag{9a}$$

$$\left(M_x^s,M_y^s,M_{xy}^s\right)=\int_{-h/2}^{h/2}\left(\sigma_x,\sigma_y,\sigma_z\right)f_1(z)zdz \tag{9b}$$

$$\left(N_x,N_y,N_{xy}\right)=\int_{-h/2}^{h/2}\left(\sigma_x,\sigma_y,\sigma_z\right)dz \tag{9c}$$

$$\left(Q_{xz}^e,Q_{yz}^e\right)=\int_{-h/2}^{h/2}\left(\sigma_{xz},\sigma_{yz}\right)dz \tag{9d}$$

$$\left(Q_{xz}^s,Q_{yz}^s\right)=\int_{-h/2}^{h/2}\left(\sigma_{xz},\sigma_{yz}\right)f_2(z)dz \tag{9e}$$

Using Eq. (2), the stress–strain relationship for a FG nanoplate is written as:

$$\begin{Bmatrix}\sigma_x\\ \sigma_y\\ \sigma_{xy}\\ \sigma_{yz}\\ \sigma_{xz}\end{Bmatrix}-\left(e_0l_i\right)^2\nabla^2\begin{Bmatrix}\sigma_x\\ \sigma_y\\ \sigma_{xy}\\ \sigma_{yz}\\ \sigma_{xz}\end{Bmatrix}=\begin{bmatrix}C_{11}&C_{12}&0&0&0\\ C_{12}&C_{22}&0&0&0\\ 0&0&C_{66}&0&0\\ 0&0&0&C_{44}&0\\ 0&0&0&0&C_{55}\end{bmatrix}\begin{Bmatrix}\varepsilon_x\\ \varepsilon_y\\ \gamma_{xy}\\ \gamma_{yz}\\ \gamma_{xz}\end{Bmatrix} \tag{10}$$

in which, C is the fourth order elasticity tensor. The components of this tensor are defined as:

$$C_{11}=\frac{E(z)}{1-\upsilon^2},C_{12}=\frac{\upsilon E(z)}{1-\upsilon^2},C_{22}=\frac{E(z)}{1-\upsilon^2},$$
$$C_{66}=G(z),C_{23}=G(z),C_{55}=G(z)$$
$$E(z)=(E_t-E_b)\left(\frac{2z+h}{2h}\right)^N,$$
$$\mathrm{G}(z)=(G_t-G_b)\left(\frac{2z+h}{2h}\right)^N, \quad (11)$$

where, E_t and E_b are Young's moduli of top and bottom layer; G_t and G_b are shear moduli of top and bottom layer of the FG nanoplate, respectively

$$\{N\}-(e_0l_i)^2\nabla^2\{N\}=[F^0]\{\varepsilon^0\}+[F^1]\{\kappa^b\}+[F^{1,s}]\{\kappa^s\} \quad (12a)$$
$$\{M^s\}-(e_0l_i)^2\nabla^2\{M^s\}=[F^{1,s}]\{\varepsilon^0\}+[F^{2,s}]\{\kappa^b\}+[F^{6,s}]\{\kappa^s\} \quad (12b)$$
$$\{M^b\}-(e_0l_i)^2\nabla^2\{M^b\}=[F^1]\{\varepsilon^0\}+[F^2]\{\kappa^b\}+[F^{2,s}]\{\kappa^s\} \quad (12c)$$
$$\{Q^s\}-(e_0a)^2\nabla^2\{Q^s\}=[H^{0,e}]\{\chi^e\}+[H^{0,s}]\{\chi^s\} \quad (12d)$$
$$\{Q^e\}-(e_0a)^2\nabla^2\{Q^e\}=[H^0]\{\chi^e\}+[H^{0,e}]\{\chi^s\} \quad (12e)$$

where,

$$\{N\}=\begin{Bmatrix}N_x\\N_y\\N_{xy}\end{Bmatrix},\ \{M^b\}=\begin{Bmatrix}M_x^b\\M_y^b\\M_{xy}^b\end{Bmatrix},\ \{M^s\}=\begin{Bmatrix}M_x^s\\M_y^s\\M_{xy}^s\end{Bmatrix},$$
$$\{Q^e\}=\begin{Bmatrix}Q_{yz}^e\\Q_{xz}^e\end{Bmatrix},\ \{Q^s\}=\begin{Bmatrix}Q_{yz}^s\\Q_{xz}^s\end{Bmatrix} \quad (13)$$

where, F_{ij}, H_{ij}, etc., are plate stiffness defined by

$$[F^0]=\begin{bmatrix}D_{11}^0&D_{12}^0&D_{16}^0\\D_{12}^0&D_{22}^0&D_{26}^0\\D_{16}^0&D_{26}^0&D_{66}^0\end{bmatrix},[F^1]=\begin{bmatrix}D_{11}^1&D_{12}^1&D_{16}^1\\D_{12}^1&D_{22}^1&D_{26}^1\\D_{16}^1&D_{26}^1&D_{66}^1\end{bmatrix},[F^2]=\begin{bmatrix}D_{11}^2&D_{12}^2&D_{16}^2\\D_{12}^2&D_{22}^2&D_{26}^2\\D_{16}^2&D_{26}^2&D_{66}^2\end{bmatrix}$$

$$[F^{1,s}]=\begin{bmatrix}D_{11}^{1,s}&D_{12}^{1,s}&D_{16}^{1,s}\\D_{12}^{1,s}&D_{22}^{1,s}&D_{26}^{1,s}\\D_{16}^{1,s}&D_{26}^{1,s}&D_{66}^{1,s}\end{bmatrix},[F^{2,s}]=\begin{bmatrix}D_{11}^{2,s}&D_{12}^{2,s}&D_{16}^{2}\\D_{12}^{2,s}&D_{22}^{2,s}&D_{26}^{2,s}\\D_{16}^{2,s}&D_{26}^{2,s}&D_{66}^{2,s}\end{bmatrix},[F^{6,s}]=\begin{bmatrix}D_{11}^{6,s}&D_{12}^{6,s}&D_{16}^{6,s}\\D_{12}^{6,s}&D_{22}^{6,s}&D_{26}^{6,s}\\D_{16}^{6,s}&D_{26}^{6,s}&D_{66}^{6,s}\end{bmatrix} \quad (14a)$$

$$[H^0]=\begin{bmatrix}D_{44}^0&D_{45}^0\\D_{45}^0&D_{55}^0\end{bmatrix},[H^{0,e}]=\begin{bmatrix}D_{44}^{0,e}&D_{45}^{0,e}\\D_{45}^{0,e}&D_{55}^{0,e}\end{bmatrix},[H^{0,s}]=\begin{bmatrix}D_{44}^{0,s}&D_{45}^{0,s}\\D_{45}^{0,s}&D_{55}^{0,s}\end{bmatrix}, \quad (14b)$$

$$D_{ij}^n=\int_{-h/2}^{h/2}C_{ij}z^n dz \quad \text{(i,j=1,2,6 , } n=0,1,2,3,4,6) \quad (15a)$$
$$\mathrm{D}_{ij}^{1,s}=-\frac{1}{4}\mathrm{D}_{ij}^1+\frac{5}{3h^2}\mathrm{D}_{ij}^3 \quad \text{(i,j=1,2,6)} \quad (15b)$$
$$\mathrm{D}_{ij}^{2,s}=-\frac{1}{4}D_{ij}^2+\frac{5}{3h^2}D_{ij}^4 \quad \text{(i,j=1,2,6)} \quad (15c)$$
$$\mathrm{D}_{ij}^{6,s}=\frac{1}{16}\mathrm{D}_{ij}^2-\frac{5}{6h^2}\mathrm{D}_{ij}^4+\frac{25}{9h^4}\mathrm{D}_{ij}^6 \quad \text{(i,j=1,2,6)} \quad (15d)$$
$$\left(\mathrm{D}_{ij}^0,\mathrm{D}_{ij}^2,\mathrm{D}_{ij}^4\right)=\int_{-h/2}^{h/2}C_{ij}\left(1,z^2,z^4\right)dz \quad \text{(i,j=4,5)} \quad (15e)$$
$$\mathrm{D}_{ij}^{0,e}=\frac{5}{4}\mathrm{D}_{ij}^0-\frac{5}{h^2}\mathrm{D}_{ij}^2 \quad \text{(i,j=4,5)} \quad (15f)$$
$$\mathrm{D}_{ij}^{0,s}=\frac{25}{16}\mathrm{D}_{ij}^0-\frac{25}{2h^2}\mathrm{D}_{ij}^2+\frac{25}{h^4}\mathrm{D}_{ij}^4 \quad \text{(i,j=4,5)} \quad (15g)$$

We now employ the Hamilton's principle to derive the governing equations. The analytical form of the principle can be expressed as [30]

$$\int_0^t\delta(U+V-T)dt=0 \quad (16)$$

where, δ represents a variation with respect to x and y. U, V, and T denote the strain energy of deformation, the potential energy of external forces, and the kinetic energy of the plate, respectively. Using Eq. (16), and summing the coefficients of δu, δv, δw_e, δw_b and δw_s, we may obtain the following governing equations

$$\delta u: \quad \frac{\partial N_x}{\partial x}+\frac{\partial N_{xy}}{\partial y}=I_0\frac{\partial^2 u}{\partial t^2} \tag{17a}$$

$$\delta v: \quad \frac{\partial N_y}{\partial y}+\frac{\partial N_{xy}}{\partial x}=I_0\frac{\partial^2 v}{\partial t^2} \tag{17b}$$

$$\delta w_b: \quad \left[\frac{\partial^2 M_x^b}{\partial x^2}+2\frac{\partial^2 M_{xy}^b}{\partial x\partial y}+\frac{\partial^2 M_y^b}{\partial y^2}\right]=I_0\left(\frac{\partial^2 w_e}{\partial t^2}+\frac{\partial^2 w_b}{\partial t^2}+\frac{\partial^2 w_s}{\partial t^2}\right)-I_2\nabla^2\frac{\partial^2 w_b}{\partial t^2} \tag{17c}$$

$$\delta w_s: \quad \left[\frac{\partial^2 M_x^s}{\partial x^2}+2\frac{\partial^2 M_{xy}^s}{\partial x\partial y}+\frac{\partial^2 M_y^s}{\partial y^2}+\frac{\partial Q_{xz}^s}{\partial x}+\frac{\partial Q_{yz}^s}{\partial y}\right]=I_0\left(\frac{\partial^2 w_e}{\partial t^2}+\frac{\partial^2 w_b}{\partial t^2}+\frac{\partial^2 w_s}{\partial t^2}\right)-\frac{I_2}{84}\nabla^2\frac{\partial^2 w_s}{\partial t^2} \tag{17d}$$

$$\delta w_e: \quad \frac{\partial Q_{xz}^e}{\partial x}+\frac{\partial Q_{yz}^e}{\partial y}=I_0\left(\frac{\partial^2 w_e}{\partial t^2}+\frac{\partial^2 w_b}{\partial t^2}+\frac{\partial^2 w_s}{\partial t^2}\right) \tag{17e}$$

where, the inertias I_0 and I_2 are defined by

$$(I_0, I_2)=\int_{-h/2}^{h/2}(1, z^2)\rho dz \tag{18}$$

in which, ρ is the mass of the nanoplate density. Substitution of Eqs.(12a-e) and(15a-g) into Eqs. (17a-e) yields the following governing equations in terms of the displacements:

$$\delta u: \quad C_{11}h\frac{\partial^2 u}{\partial x^2}+C_{12}h\frac{\partial^2 v}{\partial x\partial y}+C_{66}h\left(\frac{\partial^2 v}{\partial x\partial y}+\frac{\partial^2 u}{\partial y^2}\right)=I_0\frac{\partial^2 u}{\partial t^2}-(e_0 l_i)^2 I_0\nabla^2\left(\frac{\partial^2 u}{\partial t^2}\right) \tag{19a}$$

$$\delta v: \quad C_{22}h\frac{\partial^2 v}{\partial y^2}+C_{12}h\frac{\partial^2 u}{\partial x\partial y}+C_{66}h\left(\frac{\partial^2 u}{\partial x\partial y}+\frac{\partial^2 v}{\partial x^2}\right)=I_0\frac{\partial^2 v}{\partial t^2}-(e_0 l_i)^2\nabla^2\left(I_0\frac{\partial^2 v}{\partial t^2}\right) \tag{19b}$$

$$\begin{aligned}\delta w_b: \quad &-\left[D_{11}\frac{\partial^4 w_b}{\partial x^4}+2(D_{12}+2D_{66})\frac{\partial^4 w_b}{\partial x^2\partial y^2}+D_{22}\frac{\partial^4 w_b}{\partial y^4}\right]=I_0\left(\frac{\partial^2 w_a}{\partial t^2}+\frac{\partial^2 w_b}{\partial t^2}+\frac{\partial^2 w_s}{\partial t^2}\right)-I_2\nabla^2\frac{\partial^2 w_b}{\partial t^2}\\ &-(e_0 l_i)^2 I_0\nabla^2\left(\frac{\partial^2 w_a}{\partial t^2}+\frac{\partial^2 w_b}{\partial t^2}+\frac{\partial^2 w_s}{\partial t^2}\right)-(e_0 l_i)^2 I_2\nabla^4\frac{\partial^2 w_b}{\partial t^2}\end{aligned} \tag{19c}$$

$$\begin{aligned}\delta w_s: \quad &-\frac{1}{84}\left[D_{11}\frac{\partial^4 w_s}{\partial x^4}+2(D_{12}+2D_{66})\frac{\partial^4 w_s}{\partial x^2\partial y^2}+D_{22}\frac{\partial^4 w_s}{\partial y^4}\right]\\ &+\frac{5}{6}C_{55}h\left(\frac{\partial^2 w_a}{\partial x^2}+\frac{\partial^2 w_s}{\partial x^2}\right)+\frac{5}{6}C_{44}h\left(\frac{\partial^2 w_a}{\partial y^2}+\frac{\partial^2 w_s}{\partial y^2}\right)=I_0\left(\frac{\partial^2 w_a}{\partial t^2}+\frac{\partial^2 w_b}{\partial t^2}+\frac{\partial^2 w_s}{\partial t^2}\right)\\ &-\frac{I_2}{84}\nabla^2\frac{\partial^2 w_s}{\partial t^2}-(e_0 l_i)^2 I_0\nabla^2\left(\frac{\partial^2 w_a}{\partial t^2}+\frac{\partial^2 w_b}{\partial t^2}+\frac{\partial^2 w_s}{\partial t^2}\right)-(e_0 l_i)^2\frac{I_2}{84}\nabla^4\left(\frac{\partial^2 w_s}{\partial t^2}\right)\end{aligned} \tag{19d}$$

$$\delta w_a: \quad C_{55}h\frac{\partial^2 w_a}{\partial x^2}+\frac{5}{6}C_{55}h\frac{\partial^2 w_s}{\partial x^2}+C_{44}h\frac{\partial^2 w_a}{\partial y^2}+\frac{5}{6}C_{44}h\frac{\partial^2 w_s}{\partial y^2}=I_0\left(\frac{\partial^2 w_a}{\partial t^2}+\frac{\partial^2 w_b}{\partial t^2}+\frac{\partial^2 w_s}{\partial t^2}\right)$$
$$-\left(e_0 l_i\right)^2 I_0\nabla^2\left(\frac{\partial^2 w_a}{\partial t^2}+\frac{\partial^2 w_b}{\partial t^2}+\frac{\partial^2 w_s}{\partial t^2}\right) \qquad (19e)$$

It should be noted that when the nonlocal parameter is set to zero, $(e_0 l_i)=0$, Eq. (19a-e) reduces to that of the classical equation [31].

4. Analytical solutions for the simply supported rectangular nanoplate

We employ the Navier's method to obtain the closed form solutions associated with determining the natural frequencies of the rectangular nanoplates. Let us now consider the simply supported boundary conditions along all the edges of rectangular graphene sheets. The boundary conditions are of the form:

At edges x =0 and x = a

$$\begin{aligned} &v=w_e=w_b=w_s=\partial w_s/\partial y=0\\ &\partial w_e/\partial y=\partial w_b/\partial y=0 \qquad (20a)\\ &N_{xx}=M_{xx}^b=M_{xx}^s=0, \end{aligned}$$

At edges y =0 and y = b

$$\begin{aligned} &\left(\left[\mu\right]_{5\times5}+\omega^2\left[\lambda\right]_{5\times5}\right)\{\Delta\}_{5\times1}=0\\ &u=w_e=w_b=w_s=\partial w_s/\partial x=0\\ &\partial w_e/\partial x=\partial w_b/\partial x=0 \qquad (20b)\\ &N_{yy}=M_{yy}^b=M_{yy}^s=0, \end{aligned}$$

The following expressions of the displacements which automatically satisfy the above boundary conditions are assumed.

$$w_e=\sum_{m=1}^{\infty}\sum_{n=1}^{\infty}W_{emn}\sin(\alpha x)\sin(\beta y)\,e^{-i\omega t} \qquad (21a)$$

$$w_b=\sum_{m=1}^{\infty}\sum_{n=1}^{\infty}W_{bmn}\sin(\alpha x)\sin(\beta y)\,e^{-i\omega t} \qquad (21b)$$

$$w_s=\sum_{m=1}^{\infty}\sum_{n=1}^{\infty}W_{smn}\sin(\alpha x)\sin(\beta y)\,e^{-i\omega t} \qquad (21c)$$

$$u=\sum_{m=1}^{\infty}\sum_{n=1}^{\infty}U_{mn}\cos(\alpha x)\,\sin(\beta y)\,e^{-i\omega t} \qquad (21d)$$

$$v=\sum_{m=1}^{\infty}\sum_{n=1}^{\infty}V_{mn}\sin(\alpha x)\,\cos(\beta y)\,e^{-i\omega t} \qquad (21e)$$

In the above expressions, $\alpha=m\pi/a$ and $\beta=n\pi/b$, W_{emn}, W_{bmn}, W_{smn}, U_{mn}, V_{mn} are coefficients, and ω is the natural frequency of the nanoplate. Substituting Eqs.(21a-e) into Eqs. (19a-e), one can obtain a system of equations in the following matrix form:

$$\left(\left[\mu\right]_{5\times5}+\omega^2\left[\lambda\right]_{5\times5}\right)\{\Delta\}_{5\times1}=0 \qquad (22)$$

where,

$$\{\Delta\}=\left[U_{mn},V_{mn},W_{bmn},W_{smn},W_{emn}\right]^T \qquad (23)$$

Here, γ_{ij} and λ_{ij} are defined for the rectangular nanoplate as follows:

$$\gamma_{11}=D_{11}^0\alpha^2+D_{66}^0\beta^2,\quad \gamma_{12}=\alpha\beta\left(D_{12}^0+D_{66}^0\right),\quad \gamma_{13}=-D_{11}^1\alpha^3\ ,\quad \gamma_{14}=-D_{11}^{1,s}\alpha^3$$

$$\begin{aligned} &\gamma_{23}=D_{11}^1\beta^3\ ,\ \gamma_{24}=D_{11}^{1,s}\beta^3\ ,\ \gamma_{33}=D_{11}^2\alpha^4+2(D_{12}^2+2D_{66}^2)\alpha^2\beta^2+D_{22}^2\beta^4\\ &\gamma_{34}=D_{11}^{2,s}\alpha^4+2(D_{12}^{2,s}+2D_{66}^{2,s})\alpha^2\beta^2+D_{22}^{2,s}\beta^4\ ,\ \gamma_{22}=D_{66}^0\alpha^2+D_{22}^0\beta^2\\ &\gamma_{44}=D_{11}^{6,s}\alpha^4+2(D_{12}^{6,s}+2D_{66}^{6,s})\alpha^2\beta^2+D_{22}^{6,s}\beta^4+D_{55}^{0,s}\alpha^2+D_{44}^{0,s}\beta^2\\ &\gamma_{45}=D_{55}^{0,e}\alpha^2+D_{44}^{0,e}\beta^2\ ,\ \gamma_{55}=D_{55}^0\alpha^2+D_{44}^0\beta^2 \qquad (24)\\ &\lambda_{11}=\lambda_{22}=\lambda_{35}=\lambda_{45}=\lambda_{55}=\lambda_{34}=I_0+I_0(e_0l_i)^2(\alpha^2+\beta^2)\\ &\lambda_{33}=\left(1+(e_0l_i)^2(\alpha^2+\beta^2)\right)\left(I_0+I_2(\alpha^2+\beta^2)\right)\\ &\lambda_{44}=\left(1+(e_0l_i)^2(\alpha^2+\beta^2)\right)\left(I_0+\frac{I_2}{84}(\alpha^2+\beta^2)\right)\\ &\lambda_{12}=\lambda_{13}=\lambda_{14}=\lambda_{15}=\lambda_{21}=\lambda_{23}=\lambda_{24}=\lambda_{25}=\lambda_{31}=\lambda_{32}=\lambda_{41}=\lambda_{42}=\lambda_{51}=\lambda_{52}=0 \end{aligned}$$

For a nontrivial solution, the determinant of the coefficient matrix in Eq. (22) must be equal to zero. This provides an equation for determining the natural frequencies of the nanoplate.

4.1. *Validation and comparisonof the results obtained*

For the validation of the results obtained, comparisons are madebetween these results and those obtained from various theories for the orthotropic plate $(e_0 l_i = 0)$. In the present work, the boundary conditions along all the four edges are assumed to be simply supported. The material properties of the orthotropic nanoplate are obtained from the Ref. [32].

In Table 3, the natural frequencies calculated using the RPT theory are compared with those calculated using CPT, FSDT, and TSDT [33]for isotropic graphene sheets with the following material and geometrical properties:

The non-dimensional natural frequencies of the FG square nanoplate for different nonlocal parameters calculated by RPT are listed in Table 4. The material properties of the FG nanoplate (Table 3) are tabulated in the Table 2[11].

The comparisons of non-dimensional natural frequencies obtained by various theories as presented in Tables 1 and 3, the maximum and minimum values are observed for CPT and RPT, respectively. One can easily find from Table 4 that non-dimensional natural frequency decreases with increasing nonlocal parameter $(e_0 l_i)$. Further, this decrease is more sensitive at higher mode numbers.

In this Table, we assume that the nanoplate is isotropic, which means that material properties at a given point are the same in all directions.

5. Results and discussion

5.1. *Effect of aspect ratio on vibration of nanoplates*

The non-dimensional natural frequencies in Figs. (2-3) for isotropic and FG nanoplates are defined as: $\Omega = \omega \times h \times \sqrt{\rho / C_{11}}$

The variation in non-dimensional natural frequency of the nanoplate with the nonlocal parameter is shown in Fig. 2 for various aspect ratios a/b . Plate length is taken to be 10 nm. In this Section, we assume that the nanoplate is FG. The Young's modulus and Poisson's ratios of the FG nanoplate were presented in the previous Section. It is observedin Fig. 2 that natural frequency decreases with increasing aspect ratio from 1 to 2 as it does also with increasing nonlocal parameter from 0 nm to 2 nm while this decrease is more rapid for $a/b = 1$ than it is with $a/b = 2$. Further, the difference between RPT and CPT becomes more significant when aspect ratio decreases from 2 to 1.

5.2. *Comparison of natural frequencies of isotropic and FG nanoplates*

In order to comparethe natural frequencies of isotropic nanoplates with those of FG ones, we have plotted non-dimensional natural frequency versus nonlocal parameter for both isotropic and FG cases using CPT and RPT (See Fig.3). The length of the square nanoplate is 10 nm.Thematerial properties of isotropic graphene sheetsare $E = 1060\ Gpa,\ \upsilon = 0.25,\ \rho = 2250\ \text{kg}/m^3$. It is clear from this Figure that the natural frequencies of FG nanoplate are always smaller than their isotropic counterparts for both CPT and RPT. Also, it is observed that the results obtained by RPT are always smaller than those of CPT.

5.3. *Effect of higher modes and thickness ratio a/h on vibration of nanoplates*

To study the influence of higher modes on the vibration characteristics of rectangular nanoplates, the variation in non-dimensional natural frequency with the nonlocal parameter is shown in Fig. 4. The curves are plotted for different mode numbers.The length of the square FG nanoplate is10 nm. It is observed that the small length scale exhibits a higher effect for higher modes. This phenomenon isdue to the increasing interaction between atoms at smaller wavelengths (higher mode numbers). Further, the gap between the two curves (RPT and CPT) increases with an increase in mode number; in other words, the difference between the natural frequencies calculated by RPT and CPT increases with increasing mode number. Effect of thickness ratio a/h on the non-dimensional natural frequency of FG nanoplate for various nonlocal parameters is shown in Fig.5. It is found that natural frequencies decrease with increasing thickness ratio from 10 to 15.

5.4. . *Comparison of natural frequencies obtained by CPT and RPT*

In this Section, we consider a square FG nanoplatewith a lengthof10 nm. To investigate the difference between the two theories (RPT and CPT), we define percent

difference in non-dimensional natural frequencies calculated using RPT and CPT as follows:

Table 1: Comparison of the non-dimensional natural frequencies $\Omega = \omega \times h \times \sqrt{\rho / C_{11}}$ of an orthotropic square plate.

Mode number	m	n	Non-dimensional natural frequency Ω_{mn} for an orthotropic plate in various theories				
			Exact[34]	Reddy[35]	Srinivas[34]	CPT	**Present**
1	1	1	0.0474	0.0474	0.0474	0.0497	**0.0467**
2	1	2	0.1033	0.1033	0.1032	0.1120	**0.1021**
3	2	1	0.1188	0.1189	0.1187	0.1354	**0.1176**
4	2	2	0.1694	0.1695	0.1692	0.1987	**0.1678**
5	1	3	0.1888	0.1888	0.1884	0.2154	**0.1868**
6	3	1	0.2180	0.2184	0.2178	0.2779	**0.2149**
7	2	3	0.2475	0.2477	0.2469	0.3029	**0.2454**
8	3	2	0.2624	0.2629	0.2619	0.3418	**0.2603**
9	1	4	0.2969	0.2969	0.2959	0.3599	**0.2930**
10	4	1	0.3319	0.3330	0.3311	0.4773	**0.3251**
11	3	3	0.332	0.3326	0.331	0.4470	**0.3304**
12	2	4	0.3476	0.3479	0.3463	0.4480	**0.3443**
13	4	2	0.3707	0.3720	0.3696	0.5415	**0.3662**

Table 2: Material properties of the nanoplate.

Type of Materials	Young's Modulus	Poison's Ratio	Geometrical Properties
Isotropic	$E = 30 \times 10^6$	$\upsilon = 0.3$	a=10, a/b=1, a/h=10
FG	$E_1 = 1765$ Gpa, $E_2 = 1588$ Gpa	$\upsilon = 0.3$	$a/b = 1$, $a/h = 10$

$$\text{Percentage difference} = 100 \times \left| \frac{\omega_{CPT} - \omega_{RPT}}{\omega_{CPT}} \right|$$

The above percent difference versus aspect ratio for various mode numbers and thickness ratios are plotted in Figs. 6 and 7,respectively. Aspect ratio has a decreasing effect on percent difference and this effect vanishes after a certain aspect ratio; i.e., the difference between the two theories becomes constant beyond a certain aspect ratio. In addition, the difference between the two theories increases with increasing mode numberas already mentioned above. Finally, it is observed that the percent difference decreases with an increase in the thickness ratio from 10 to 20.

Table 3: Comparison of the non-dimensional natural frequencies $\Omega = \omega \times h \times \sqrt{\rho / G}$ of an isotropic square nanoplate.

frequencies	$(e_0 l_i)^2$	TSDT[33]	FSDT[33]	CPT	**Present**
ω_{11}	0	0.0935	0.0930	0.0963	**0.0930**
	1	0.0854	0.0850	0.0880	**0.0850**
	2	0.0791	0.0788	0.0816	**0.0788**
	3	0.0741	0.0737	0.0763	**0.0737**
	4	0.0699	0.0696	0.0720	**0.0695**
	5	0.0663	0.0660	0.0 683	**0.0660**
ω_{22}	0	0.3458	0.3414	0.3853	**0.3406**
	1	0.2585	0.2552	0.288	**0.2546**
	2	0.2153	0.2126	0.2399	**0.2121**
	3	0.1884	0.186	0.2099	**0.1856**
	4	0.1696	0.1674	0.1889	**0.1670**
	5	0.1555	0.1535	0.1732	**0.1531**
ω_{33}	0	0.702	0.6889	0.8669	**0.6839**
	1	0.4213	0.4134	0.5202	**0.4105**
	2	0.329	0.3228	0.4063	**0.3205**
	3	0.279	0.2738	0.3446	**0.2719**
	4	0.2466	0.242	0.3045	**0.2402**
	5	0.2233	0.2191	0.2757	**0.2176**

Table 4: The non-dimensional natural frequencies $\Omega = \omega \times h \times \sqrt{\rho / C_{11}}$ of an FG nanoplate calculated by RPT.

Mode number	*m*	*n*	$e_0 l_i$ (nm)				
			0	0.5	1	1.5	**2**
1	1	1	0.0541	0.0528	0.0494	0.0450	**0.0404**
2	1	2	0.1270	0.1199	0.1040	0.0875	**0.0737**
3	2	1	0.1307	0.1233	0.1070	0.0900	**0.0758**
4	2	2	0.1985	0.1814	0.1484	0.1191	**0.0973**
5	1	3	0.2369	0.2122	0.1681	0.1320	**0.1065**
6	3	1	0.2453	0.2197	0.1740	0.1367	**0.1103**
7	2	3	0.3013	0.2622	0.1994	0.1528	**0.1217**
8	3	2	0.3061	0.2664	0.2026	0.1553	**0.1236**
9	1	4	0.3730	0.3131	0.2280	0.1707	**0.1343**
10	4	1	0.3861	0.3241	0.2360	0.1767	**0.1390**
11	3	3	0.3997	0.3326	0.2399	0.1788	**0.1404**
12	2	4	0.4301	0.3519	0.2494	0.1844	**0.1442**
13	4	2	0.4398	0.3599	0.2550	0.1886	**0.1475**

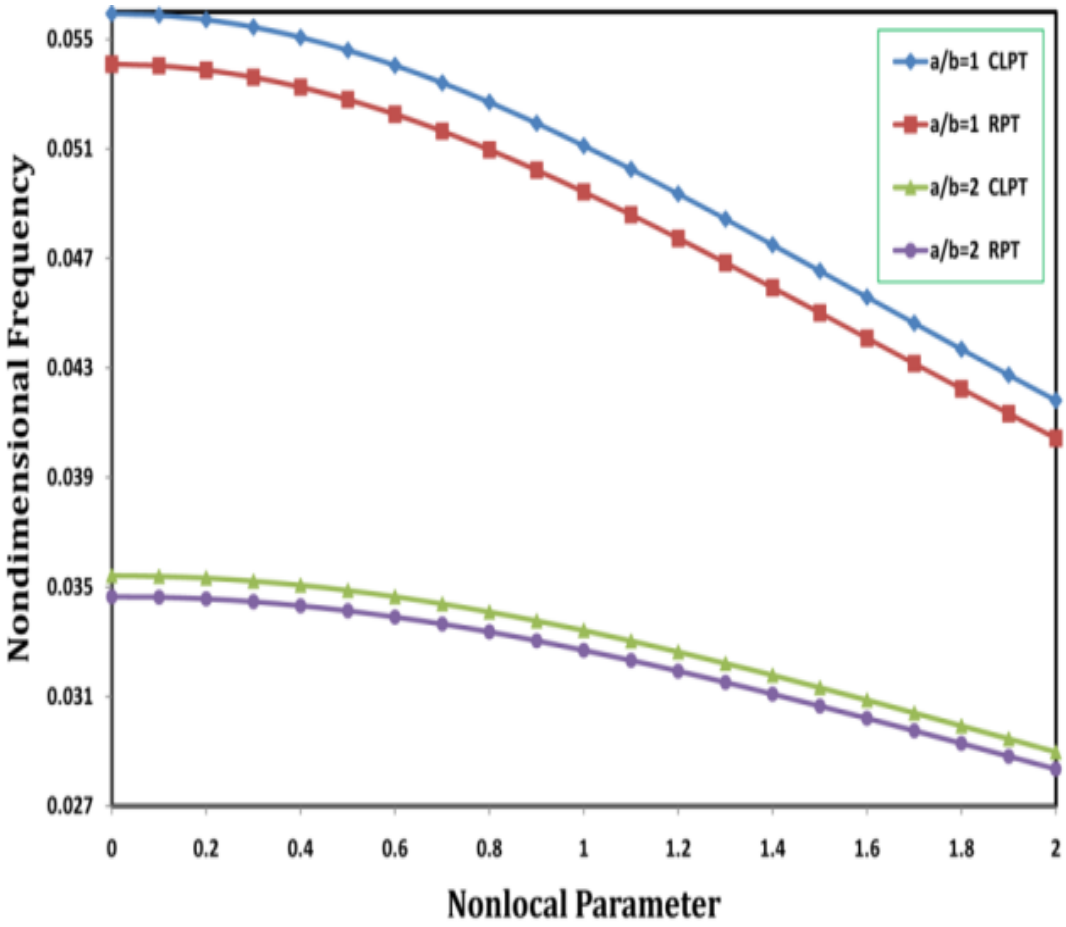

Fig. 2. Variation in non-dimensional frequency with nonlocal parameter for different aspect ratios

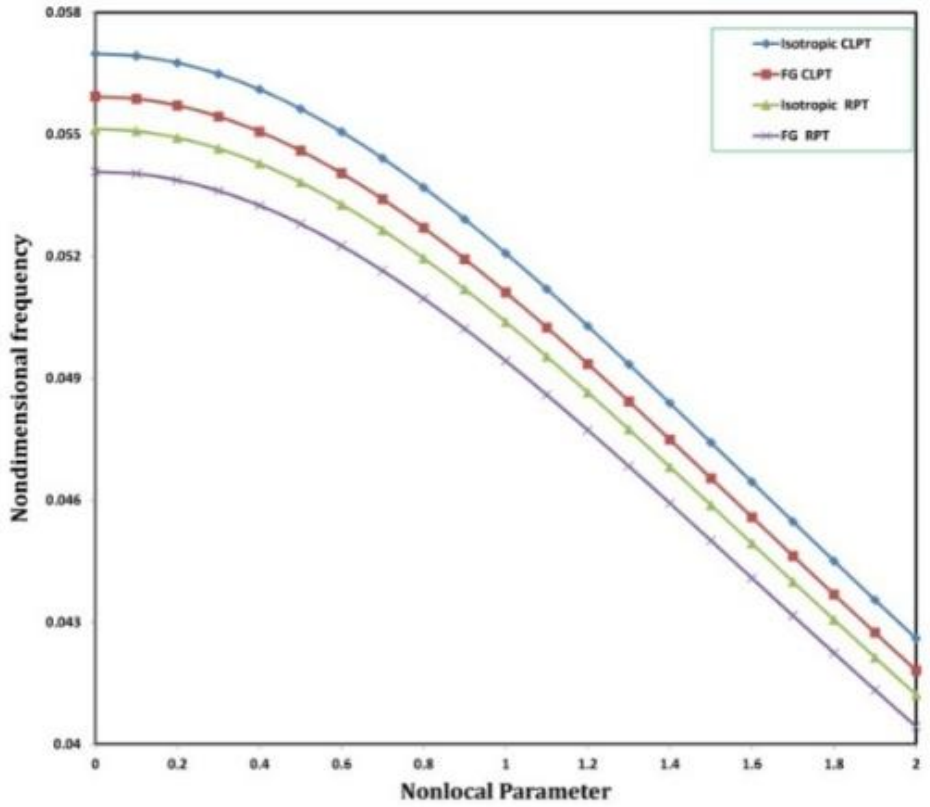

Fig. 3. Variation in non-dimensional frequency with nonlocal parameter for isotropic and FG nanoplates

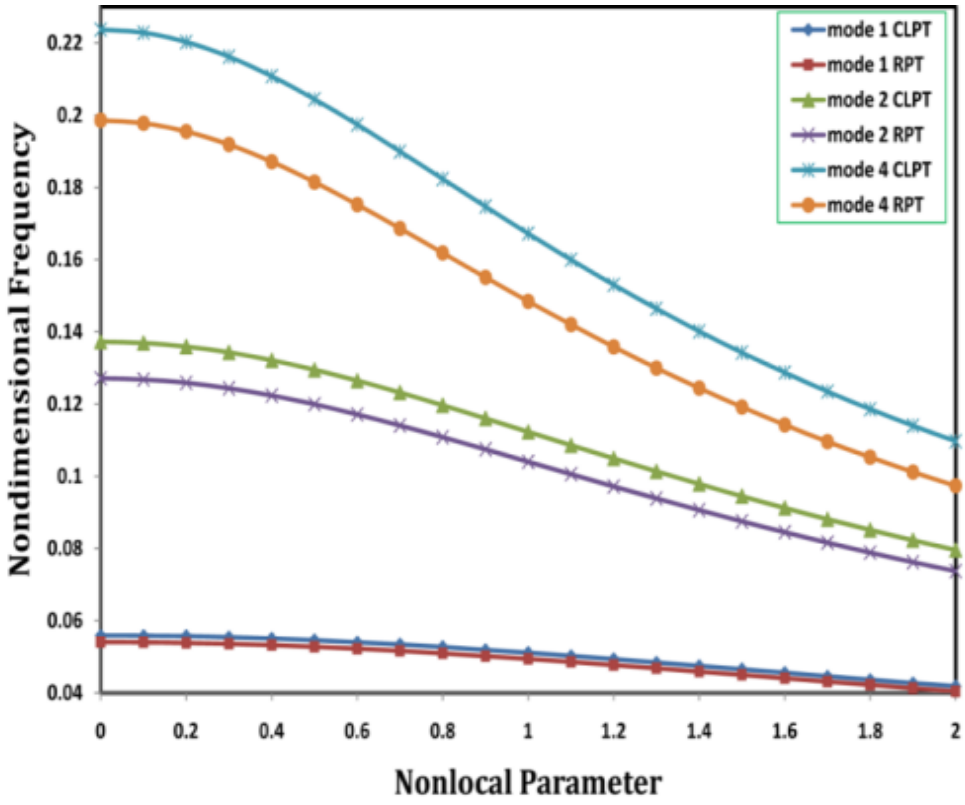

Fig. 4.Variation in non-dimensional frequency with nonlocal parameter for different mode frequencies.

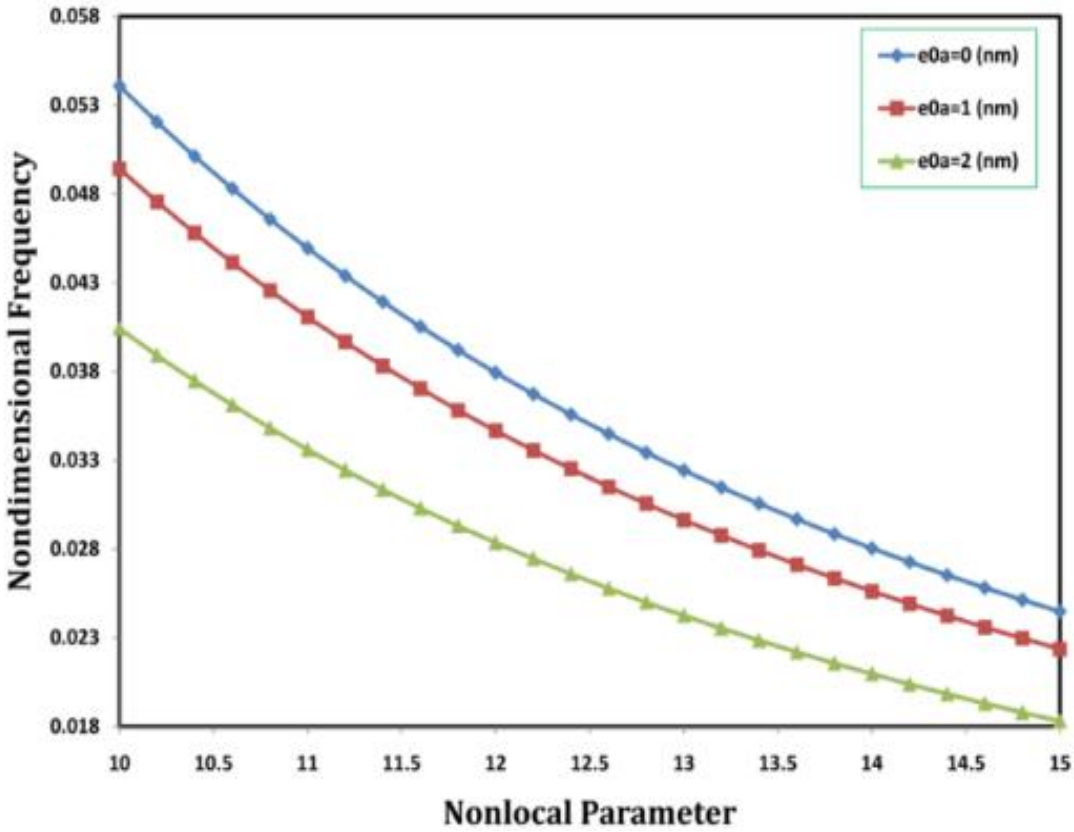

Fig. 5. Variation in non-dimensional frequency with thickness ratio for different nonlocal parameters.

6. Conclusions

Based on the two-variable refined plate theory and the nonlocal plate theory, the small scale effect on the free vibration of FG rectangular nanoplates was investigated. The boundary conditions along all the four edges were assumed to be simply supported. The governing equations of the plate were solved using the Navier's method. The effects of nonlocal parameter, thickness ratio, aspect ratio, and mode number on the natural frequencies of FG nanoplate were investigated. The following conclusions may be drawn from the findings of the present study:

(1). Natural frequency decreases with aspect ratio increasing from 1 to 2.

(2). The natural frequencies of FG nanoplates are always found to be smaller than their isotropic counterparts for both CPT and RPT and the results obtained by RPT are always found to be smaller than those of CPT.

(3). The effect of small length scale is higher for higher modes. Furthermore, the difference between the results from the two theories increases with increasing mode number.

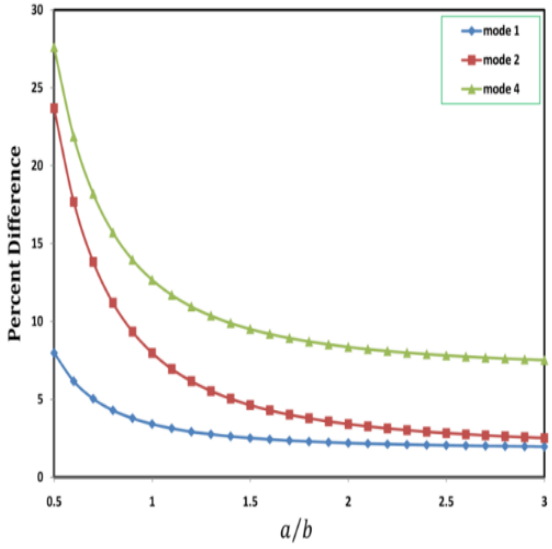

Fig. 6. Percent difference in non-dimensional frequency between RPT and CLPT with aspect ratio for different mode frequencies

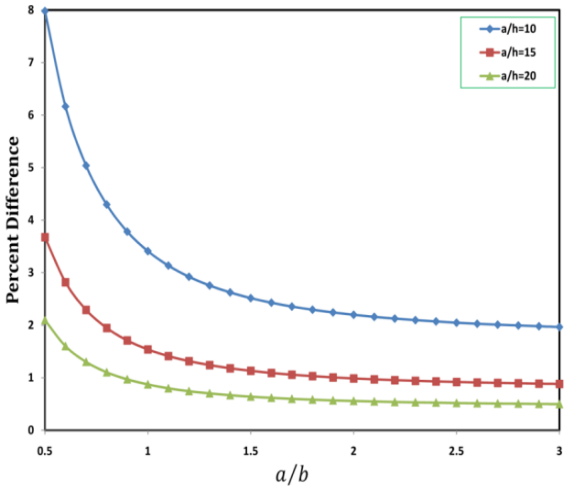

Fig. 7. Percent difference in non-dimensional frequency between RPT and CLPT with aspect ratio for different thickness ratios

7. References

[1] M. A. Eltaher, F. F. Mahmoud, A. E. Assie, E. I. Meletis, Coupling effects of nonlocal and surface energy on vibration analysis of nanobeams, *Applied Mathematics and Computation*, Vol. 224, pp. 760-774, 11/1/, 2013.

[2] M. A. Eltaher, M. A. Agwa, F. F. Mahmoud, Nanobeam sensor for measuring a zeptogram mass, *International Journal of Mechanics and Materials in Design*, Vol. 12, No. 2, pp. 211-221, 2016.

[3] M. Z. Nejad, A. Hadi, A. Rastgoo, Buckling analysis of arbitrary two-directional functionally graded Euler–Bernoulli nano-beams based on nonlocal elasticity theory, *International Journal of Engineering Science*, Vol. 103, pp. 1-10, 2016.

[4] M. Z. Nejad, A. Hadi, Non-local analysis of free vibration of bi-directional functionally graded Euler–Bernoulli nano-beams, *International Journal of Engineering Science*, Vol. 105, pp. 1-11, 2016.

[5] M. Safarabadi, M. Mohammadi, A. Farajpour, M. Goodarzi, Effect of surface energy on the vibration analysis of rotating nanobeam, *Journal of Solid Mechanics*, Vol. 7, No. 3, pp. 299-311, 2015.

[6] M. Danesh, A. Farajpour, M. Mohammadi, Axial vibration analysis of a tapered nanorod based on nonlocal elasticity theory and differential quadrature method, *Mechanics Research Communications*, Vol. 39, No. 1, pp. 23-27, 2012.

[7] H. Moosavi, M. Mohammadi, A. Farajpour, S. Shahidi, Vibration analysis of nanorings using nonlocal continuum mechanics and shear deformable ring theory, *Physica E: Low-dimensional Systems and Nanostructures*, Vol. 44, No. 1, pp. 135-140, 2011.

[8] A. Farajpour, A. Shahidi, M. Mohammadi, M. Mahzoon, Buckling of orthotropic micro/nanoscale plates under linearly varying in-plane load via nonlocal continuum mechanics, *Composite Structures*, Vol. 94, No. 5, pp. 1605-1615, 2012.

[9] M. Mohammadi, A. Moradi, M. Ghayour, A. Farajpour, Exact solution for thermo-mechanical vibration of orthotropic mono-layer graphene sheet embedded in an elastic medium, *Latin American Journal of Solids and Structures*, Vol. 11, No. 3, pp. 437-458, 2014.

[10] M. Mohammadi, A. Farajpour, M. Goodarzi, R. Heydarshenas, Levy type solution for nonlocal thermo-mechanical vibration of orthotropic mono-layer graphene sheet embedded in an elastic medium, *Journal of Solid Mechanics*, Vol. 5, No. 2, pp. 116-132, 2013.

[11] M. Mohammadimehr, B. R. Navi, A. G. Arani, Modified strain gradient Reddy rectangular plate model for biaxial buckling and bending analysis of double-coupled piezoelectric polymeric nanocomposite reinforced by FG-SWNT, *Composites Part B: Engineering*, Vol. 87, pp. 132-148, 2016.

[12] M. Mohammadi, A. Farajpour, A. Moradi, M. Ghayour, Shear buckling of orthotropic rectangular graphene sheet embedded in an elastic medium in thermal environment, *Composites Part B: Engineering*, Vol. 56, pp. 629-637, 2014.

[13] M. Mohammadi, A. Farajpour, M. Goodarzi, F. Dinari, Thermo-mechanical vibration analysis of annular and circular graphene sheet embedded in an elastic medium, *Latin American Journal of Solids and Structures*, Vol. 11, No. 4, pp. 659-682, 2014.

[14] A. Daneshmehr, A. Rajabpoor, A. Hadi, Size dependent free vibration analysis of nanoplates made of functionally graded materials based on nonlocal elasticity theory with high order theories, *International Journal of Engineering Science*, Vol. 95, pp. 23-35, 2015.

[15] A. C. Eringen, On differential equations of nonlocal elasticity and solutions of screw dislocation and surface waves, *Journal of Applied Physics*, Vol. 54, No. 9, pp. 4703-4710, 1983.

[16] R. Nazemnezhad, S. Hosseini-Hashemi, Free vibration analysis of multi-layer graphene nanoribbons incorporating interlayer shear effect via molecular dynamics simulations and nonlocal elasticity, *Physics Letters A*, Vol. 378, No. 44, pp. 3225-3232, 2014.

[17] H. G. Craighead, Nanoelectromechanical systems, *Science*, Vol. 290, No. 5496, pp. 1532-6, Nov 24, 2000. eng

[18] R. Ansari, B. Arash, H. Rouhi, Vibration characteristics of embedded multi-layered graphene sheets with different boundary conditions via nonlocal elasticity, *Composite Structures*, Vol. 93, No. 9, pp. 2419-2429, 2011.

[19] J. N. Reddy, Nonlocal nonlinear formulations for bending of classical and shear deformation theories of beams and plates, *International Journal of Engineering Science*, Vol. 48, No. 11, pp. 1507-1518, 11//, 2010.

[20] A. Assadi, B. Farshi, Size dependent stability analysis of circular ultrathin films in elastic medium with consideration of surface energies, *Physica E: Low-dimensional Systems and Nanostructures*, Vol. 43, No. 5, pp. 1111-1117, 3//, 2011.

[21] A. C. Eringen, 2002, *Nonlocal Continuum Field Theories*, Springer New York,

[22] M. Aydogdu, Axial vibration analysis of nanorods (carbon nanotubes) embedded in an elastic medium using nonlocal elasticity, *Mechanics Research Communications*, Vol. 43, pp. 34-40, 2012.

[23] M. Mohammadi, A. Farajpour, M. Goodarzi, H. Mohammadi, Temperature effect on vibration analysis of annular graphene sheet embedded on visco-Pasternak foundation, *Journal of Solid Mechanics*, Vol. 5, No. 3, pp. 305-323, 2013.

[24] M. Mohammadi, M. Goodarzi, M. Ghayour, S. Alivand, Small scale effect on the vibration of orthotropic plates embedded in an elastic medium and under biaxial in-plane pre-load via nonlocal elasticity theory, *Journal of Solid Mechanics*, Vol. 4, No. 2, pp. 128-143, 2012.

[25] M. Mohammadi, A. Farajpour, M. Goodarzi, Numerical study of the effect of shear in-plane load on the vibration analysis of graphene sheet embedded in an elastic medium, *Computational Materials Science*, Vol. 82, pp. 510-520, 2014.

[26] A. Hadi, A. Rastgoo, A. Daneshmehr, F. Ehsani, Stress and strain analysis of functionally graded rectangular plate with exponentially varying properties, *Indian Journal of Materials Science*, Vol. 2013, 2013.

[27] M. Z. Nejad, A. Hadi, Eringen's non-local elasticity theory for bending analysis of bi-directional functionally graded Euler–Bernoulli nano-beams, *International Journal of Engineering Science*, Vol. 106, pp. 1-9, 2016.

[28] M. Hosseini, M. Shishesaz, K. N. Tahan, A. Hadi, Stress analysis of rotating nano-disks of variable thickness made of functionally graded materials, *International Journal of Engineering Science*, Vol. 109, pp. 29-53, 2016.

[29] Ö. Civalek, Ç. Demir, Bending analysis of microtubules using nonlocal Euler–Bernoulli beam theory, *Applied Mathematical Modelling*, Vol. 35, No. 5, pp. 2053-2067, 5//, 2011.

[30] S. R. Asemi, A. Farajpour, Vibration characteristics of double-piezoelectric-nanoplate-systems, *Micro & Nano Letters, IET*, Vol. 9, No. 4, pp. 280-285, 2014.

[31] R. Shimpi, H. Patel, A two variable refined plate theory for orthotropic plate analysis, *International Journal of Solids and Structures*, Vol. 43, No. 22, pp. 6783-6799, 2006.

[32] B. Akgöz, Ö. Civalek, Free vibration analysis of axially functionally graded tapered Bernoulli–Euler microbeams based on the modified couple stress theory, *Composite Structures*, Vol. 98, pp. 314-322, 2013.

[33] R. Aghababaei, J. Reddy, Nonlocal third-order shear deformation plate theory with application to bending and vibration of plates, *Journal of Sound and Vibration*, Vol. 326, No. 1, pp. 277-289, 2009.

[34] S. Srinivas, A. Rao, Bending, vibration and buckling of simply supported thick orthotropic rectangular plates and laminates, *International Journal of Solids and Structures*, Vol. 6, No. 11, pp. 1463-1481, 1970.

[35] J. Reddy, A refined nonlinear theory of plates with transverse shear deformation,

International Journal of solids and structures, Vol. 20, No. 9-10, pp. 881-896, 1984.